ACS Photonics

Article

pubs.acs.org/journal/apchd5

Nanomovement of Azo Polymers Induced by Longitudinal Fields

Hidekazu Ishitobi,*[,†,‡] Issei Nakamura,[§] Taka-aki Kobayashi,[‡] Norihiko Hayazawa,[§] Zouheir Sekkat,[⊥,∥,#] Satoshi Kawata,[‡,§] and Yasushi Inouye[†,‡]

[†]Graduate School of Frontier Biosciences, Osaka University, 1-3 Yamadaoka, Suita, Osaka 565-0871, Japan

[‡]Department of Applied Physics, Osaka University, 2-1 Yamadaoka, Suita, Osaka 565-0871, Japan

[§]Near-field Nanophotonics Research Team, RIKEN, 2-1 Hirosawa, Wako, Saitama 351-0198, Japan

[⊥]Optics & Photonics Center, Moroccan Foundation for Advanced Science, Innovation and Research, Rabat, Morocco

[∥]Faculty of Sciences, University Mohamed V-Agdal, Rabat, Morocco

[#]Hassan II Academy of Science & Technology, Rabat, Morocco

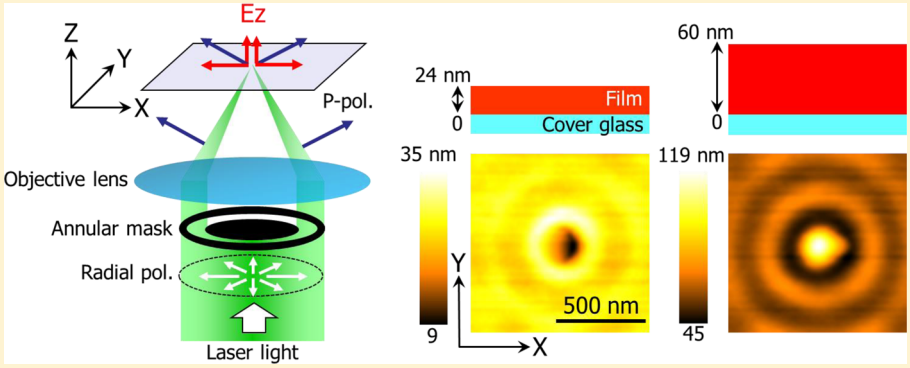

ABSTRACT: Surface deformations were induced in azo-polymer films by a focused laser spot that has a longitudinal field (E_z). We found that the deformation patterns induced by E_z were strongly dependent on polymer film thickness. The polymer formed a dip at the center of the focused spot when the film thickness is thinner than 37 nm, while the polymer formed a protrusion when the film thickness is thicker than 37 nm. These results imply that upward and downward forces are competing inside the polymer film, and the balance between them finally decides the surface topology (dip versus protrusion) of the film. We also found that the deformation patterns were dependent on the refractive index of the material on the film. We calculated the light field distribution inside the polymer film, and by comparing the experimental results we found that both anisotropic photofluidic force and optical gradient force might play important roles in the polymer movement. In addition, we found by changing the wavelength of the irradiation light that optical gradient force exerted on not the side-chain of the azobenzene moiety but the main chain of the polymer contributes to the polymer movement.

KEYWORDS: *light-induced mass transport, cis−trans isomerization, radial polarization, optical gradient force, anisotropic photofluidic force*

Light-induced surface deformations in azobenzene-containing polymer films have attracted much attention owing to applications in micro/nanofabrication[1,2] and in subdiffraction imaging of optical near-fields.[3,4] It is well known that such patterns reflect the state of the incident light polarization and the light intensity distribution.[5] Trans ↔ cis photoselective isomerization and molecular reorientation play important roles in the deformation process. Light-induced mass movement in azo polymers have triggered many studies to understand the mechanism of polymer migration, and most of the studies have focused on surface relief gratings (SRGs), which are fabricated by the interference pattern of two coherent laser beams.[6−15] There are several reports on surface deformations that are induced by a single focused laser spot.[16−22] The use of a single focused laser spot has the advantage of better understanding the underlying mechanism of light-induced mass movement than the SRGs because the impulsive response of polymer movement can be directly measured. Recently, Ambrosio et al. reported on light-induced spiral mass transport in azo-polymer films under vortex-beam illumination, where they found that the induced patterns are sensitive to the vortex topological charge and to the wavefront handedness.[22] Polymer movement in azo polymers induced by light whose polarization is parallel to the film surface (lateral fields, $E_{x,y}$) could be qualitatively explained by anisotropic photofluidic force,[23] though its origin is still under investigation. Few studies have been reported concerning azo-polymer mass movement induced by longitudinal fields (E_z). For applications in subdiffraction imaging of

Received: September 24, 2013
Published: February 12, 2014

optical near-fields, the study on polymer movement induced by E_z is important because evanescent near-fields are generally polarized in the longitudinal direction. Thus it is essential to understand the mechanism of polymer movement induced by E_z. Gilbert et al. observed surface deformations on 40 nm thickness azo-polymer films induced by E_z that was created by radial polarization, and they found that a protrusion was induced at the center of the focused spot.[17] Grosjean et al. observed surface deformations on 100 nm thickness azo-polymer films induced by E_z that was created by a radially polarized Bessel beam, and they also found that a protrusion was induced at the center of the focused spot.[18,20] In these reports, the weight ratio of E_z to $E_{x,y}$ was not so large, so both E_z and $E_{x,y}$ are mixed inside the focused spot, a feature that makes it difficult to clearly understand the mechanism of polymer movement by E_z.

In this paper, we report on surface deformations of azo-polymer films by irradiation with a single tightly focused laser beam that has strong E_z compared with $E_{x,y}$, in which we found that the deformation patterns were strongly dependent on the polymer film thickness. We will discuss the effect of film thickness on deformation patterns by changing the film thickness and manipulating the refractive index of the material on the polymer film. In addition, by comparing calculations of light field distributions inside a polymer film with experimental observations, it will be shown that anisotropic photofluidic force and optical gradient force might play important roles in light-induced polymer movement. We will also discuss irradiation wavelength dependence that is related to the direction of optical gradient force.

EXPERIMENTAL SECTION

We prepared thin films of poly(Disperse Red 1 methacrylate) (PMA-DR1, product No. 579009, Aldrich; T_g = 82 °C) by spin coating from a chloroform solution onto microscopic cover glass. The film thickness was controlled by changing the rotation speed of the spin coating. The remaining solvent was removed by heating the films for an hour at 100 °C. The chemical structure and the absorption spectrum of the film are shown in Figure 1. Disperse Red 1 (DR1) is a nonlinear optical azo dye that is well known for its trans ↔ cis photoisomerization and for its ability to undergo efficient orientation and trigger polymer movement when it is excited by polarized light.[24] The orientation effect is due to the highly anisometric nature of its polarizability tensor (rodlike molecule).[25]

Figure 2 shows the optical setup for inducing and measuring polymer movement by E_z. The irradiation light source was a linearly polarized 532 light from a diode pumped frequency doubled laser (Sapphire 532, Coherent Japan). Radial polarization was created by a 12 divided half-wave plate (SWP-532, Photonic Lattice Inc.) in which each element has different directions of crystal axes.[26] With this specially designed phase plate, linear polarization can be converted to radial polarization. The radially polarized laser beam was focused by an objective lens (NA = 1.4) (Plan Apo 100×, Nikon). An annular mask was used to increase the ratio of E_z to $E_{x,y}$. We found by calculations of light field distributions in the presence of the interface between air (n = 1.0) and polymer (n = 1.5) that an NA of 1.0 has the highest ratio of E_z to $E_{x,y}$. We also found that an NA more than 1.0 has a higher component of E_z in the illumination, but the final E_z inside the focused spot is decreased by destructive interference between incident light and reflected light at the boundary of the polymer film and air. Considering

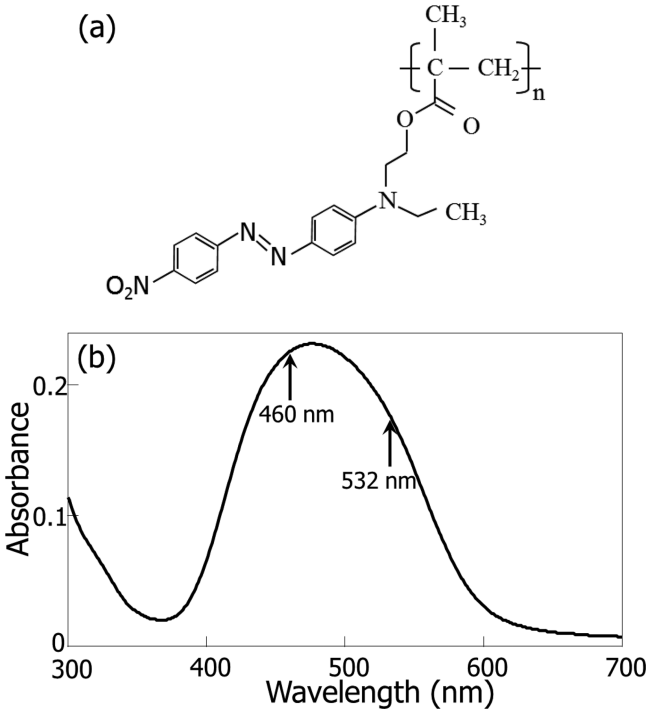

Figure 1. (a) Chemical structure and (b) absorption spectrum of the trans-DR1-PMA thin film. The wavelength of excitation is indicated.

the throughput of the transmitted light and the diffraction effect caused by the narrow annular mask, we selected the annular size that corresponds to the NA of 1.0 to 1.2. By using this annular mask, we have succeeded in increasing the ratio of E_z to $E_{x,y}$ ($|E_z|^2/|E_{x,y}|^2$) to 5 (see Figure 3), while without the annular mask the ratio is 2. In addition to increasing the ratio of E_z to $E_{x,y}$, annular illumination has another advantage: that we can rule out the dependence of deformation patterns on the focused laser position along the optical axis because annular illumination ideally creates a Bessel beam, which has a long focal depth.[18] Actually we experimentally confirmed that the deformation patterns are independent of the focused laser position along the optical axis (not shown). A computer-controlled piezo stage (P-517.3CD, Physik Instrumente) was used to control the position of the focused laser spot in three dimensions. The induced surface deformations of the films were measured by an atomic force microscope (AFM) (SPA-400, SEIKO Instruments Inc.). The AFM was operated in the tapping mode using a Si cantilever to eliminate the mechanical deformation of the films by the cantilever itself. For investigating irradiation wavelength dependence that is related to the direction of optical gradient force, we used a linearly polarized 460 nm light from a diode-pumped frequency doubled laser (Sapphire 460 LP, Coherent Japan) for the irradiation light source besides the 532 nm laser. We also used a liquid crystal based polarization converter (RADPOL4, ARCoptix Inc.) for creating radial polarization of 460 nm.

RESULTS AND DISCUSSION

Figure 4 shows the AFM images of the surface deformations induced by E_z in the films of different thicknesses. The irradiation intensity and the exposure time were 2.0 W/cm^2 and 30 s, respectively, and the laser beam was focused on the film surface. These irradiation conditions were the same as other experiments discussed later except the systematic study

dx.doi.org/10.1021/ph400052b | ACS Photonics 2014, 1, 190−197

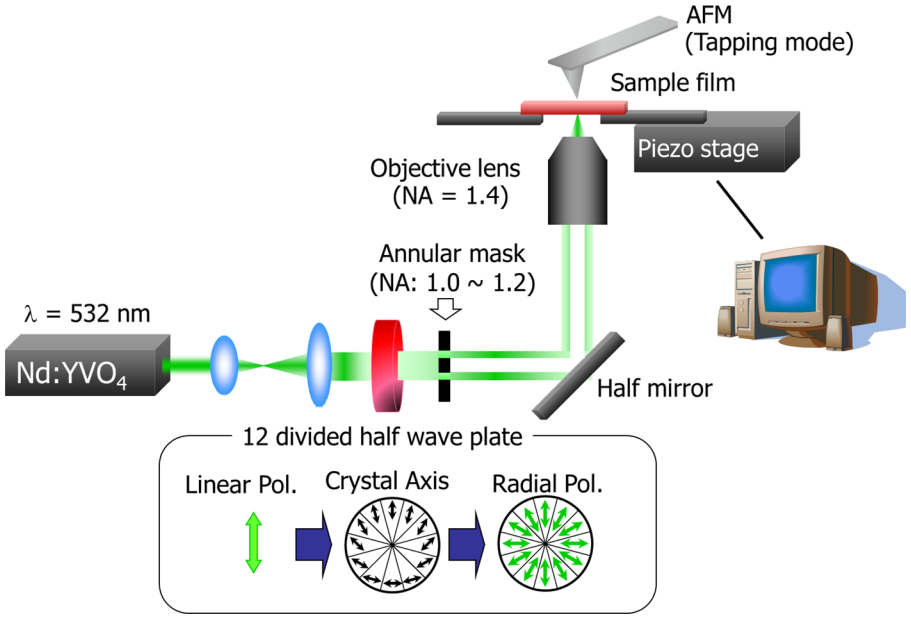

Figure 2. Optical setup for inducing and measuring polymer movement by E_z.

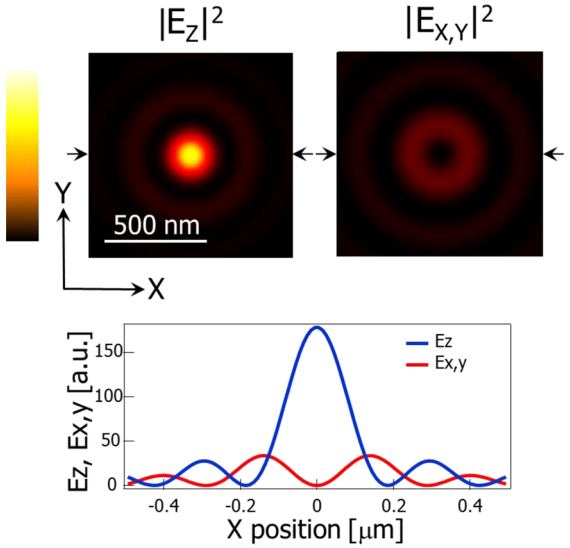

Figure 3. Calculated distributions of squared electric field components created by a tightly focused radially polarized laser beam in the presence of the interface between air (n = 1.0) and polymer (n = 1.5). The components of electric fields of (a) E_z and (b) $E_{x,y}$ are shown. x and y are parallel to the film surface, and z is the optical axis. The distributions were calculated in the xy in-plane, which is located 5 nm below the interface. The line plots of E_z and $E_{x,y}$ are also shown. The positions of each plot correspond to the directions that are between the arrows indicated in the calculated images.

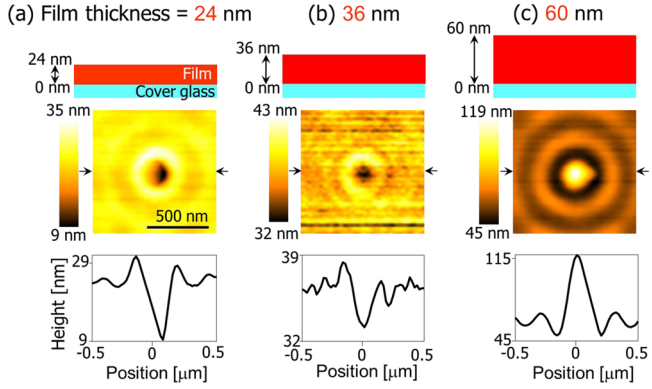

Figure 4. AFM images of the surface deformation induced by E_z in the (a) 24 nm, (b) 36 nm, and (c) 60 nm thick films. Schematics of cross sections of the films are show for describing the relationship between cover glass surfaces and film thicknesses. The line plots of the surface deformations for each thickness are also shown. The positions of each plot correspond to the directions that are between the arrows indicated in the AFM images.

(Figures 7, 8). It is clearly shown in the figure that the deformation patterns are strongly dependent on the polymer film thickness. In the 24 nm thick film (a), a dip was induced at the center of the focused spot. In contrast, in the 60 nm thick film (c), a protrusion was induced. It is reasonable to think that the direction of the polymer movements is parallel to the polarization direction. Thus, the dip and the protrusion were induced by downward and upward forces that are parallel to the polarization direction (z), respectively. At the intermediate film thickness (36 nm) between them (b), the dip was induced where the depth of the dip was small compared with that induced in the 24 nm thick film. These results imply the existence of a film thickness that corresponds to no deformation, where upward and downward forces are balanced.

To explore the film thickness that corresponds to no deformation, we induced polymer movement in a film where the film thickness is slightly modulated in the same sample film (see Figure 5). In the figure, from the left to the right, the film thickness is gradually increased, i.e., (a) 36 nm, (b) 37 nm, (c) 43 nm. At the 36 nm film thickness (a), a dip was induced at the center of the focused spot, while at the 43 nm film thickness (c), a protrusion was induced at the center of the focused spot. It is interesting to see that at the 37 nm film thickness (c) no deformation was induced. This result indicates the existence of two competing upward and downward forces inside the polymer film, and the balance between them finally decides the surface topology (dip versus protrusion) of the film.

This film thickness dependent polymer movement is inherent for E_z. Figure 6 shows film thickness dependence of

dx.doi.org/10.1021/ph400052b | ACS Photonics 2014, 1, 190−197

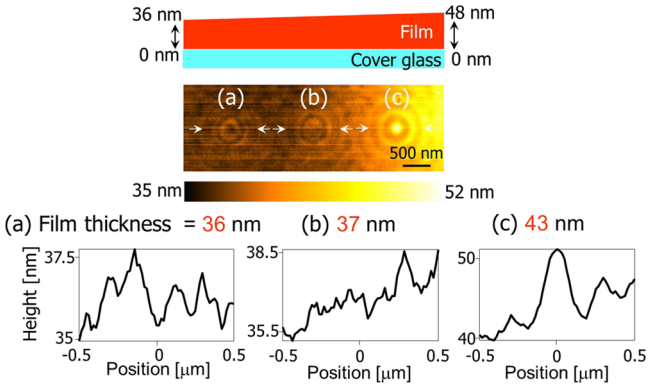

Figure 5. AFM image of the surface deformations induced by E_z where the film thickness is slightly modulated in the same sample film. In the figure, from the left to the right, the film thickness is gradually increased, i.e., (a) 36 nm, (b) 37 nm, (c) 43 nm. Schematics of cross sections of the film are shown to describe the relationship between cover glass surfaces and film thicknesses. The line plots of the surface deformations for each thickness are also shown. The positions of each plot correspond to the directions that are between the arrows indicated in the AFM images.

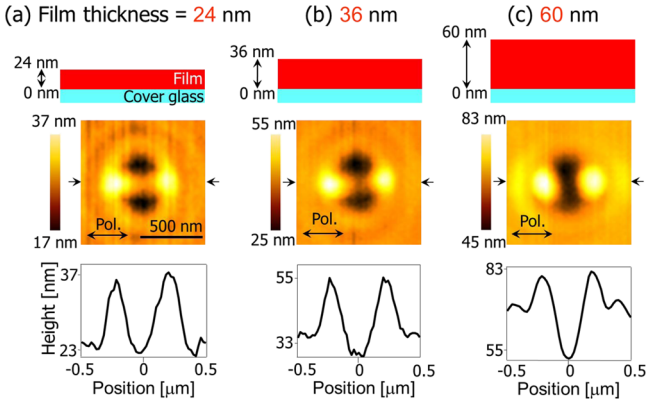

Figure 6. AFM images of the surface deformation induced by E_x in the (a) 24 nm, (b) 36 nm, and (c) 60 nm thick films. Schematics of cross sections of the films are shown to describe the relationship between cover glass surfaces and film thicknesses. The line plots of the surface deformations for each thickness are also shown. The positions of each plot correspond to the directions that are between the arrows indicated in the AFM images.

polymer movement induced by lateral fields. The sample films were irradiated with linear polarization (E_x) instead of radial polarization. In addition, by removing the annular mask, the full NA components of 0 to 1.4 were used. With the full NA components, the dominant component of the fields in the focused spot is E_x.[19] We prepared the same film thickness samples as Figure 4 (24, 36, and 60 nm). It is clearly shown in this figure that the deformation patterns were almost the same in all different thickness films, although the modulation depth was increased for the thicker film. Thus it is clear that there is no obvious film thickness dependence for lateral fields in terms of deformation patterns. It was reported that for the irradiation with E_x the polymer moves in the polarization direction from high- to low-intensity regions and then forms a dip at the center of the focused spot and two lobes in the polarization direction.[16,17,19,22] The polymer movement induced by E_x is characterized by anisotropic photofluidic force. It should be noted that the height of the polymer film at the center of the

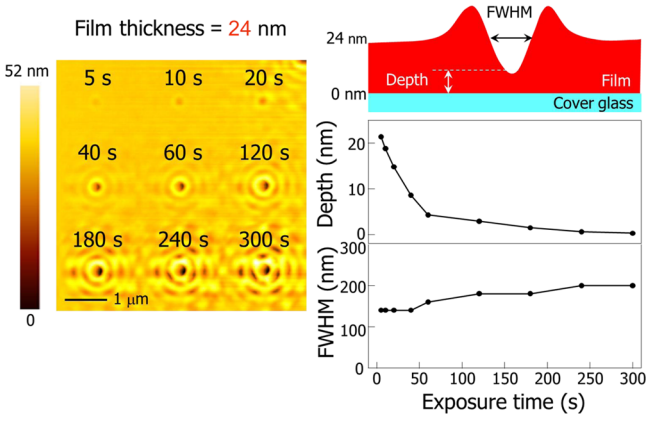

Figure 7. Size dependence of the surface deformation on the exposure time in the 24 nm thick film. The AFM image of the deformation patterns is shown in the left of the figure, and the definitions of the depth and the fwhm are indicated in the upper right. Scatters are experimental data, and solid lines are exponential empirical theoretical fits.

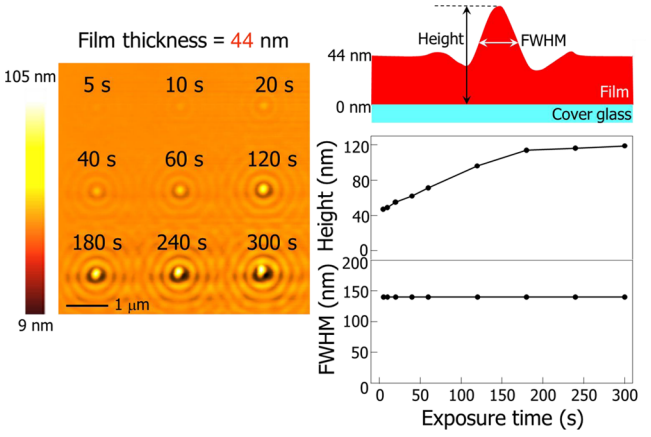

Figure 8. Size dependence of the surface deformation on the exposure time in the 44 nm thick film. The AFM image of the deformation patterns is shown in the left of the figure, and the definitions of the depth and the fwhm are indicated in the upper right. Scatters are experimental data, and solid lines are exponential empirical theoretical fits.

focused spot is not a minimum; instead, there are two minima along the direction perpendicular to the incident polarization. Actually this phenomenon was observed in the early stage of the polymer movements, e.g., 60 s irradiation, which is the case in this figure. We found, by increasing the irradiation time, for example, to 300 s, this phenomenon becomes less noticeable, and the polymer movement that induces the dip at the center and the two lobes in the x-direction becomes dominant. Currently the detailed mechanism of this phenomenon is still unclear, so we will study this phenomenon in future work.

We studied the dependence of the size of the light-induced deformation on the exposure time. The deformation pattern was studied by changing exposure times according to the series 5 to 300 s and fixing the irradiation intensity at 2.0 W/cm^2. Figures 7 and 8 show the dependence of the depth (or height) and the full width at half-maximum (fwhm) of the deformation patterns on the exposure time for the 24 and the 44 nm thick films, respectively. It is expected from the experimental results in Figures 4 and 5 that the 24 and the 44 nm thick films form a dip and a protrusion in the center of a focused spot. The depth

dx.doi.org/10.1021/ph400052b | ACS Photonics 2014, 1, 190−197

(or height) is defined as the difference between the bottom (or top) of the central dip (or protrusion) and the surface of the cover glass, as shown in the figures. It is interesting to see that the depth (or the height) was decreased (or increased) as the exposure time was increased, but the fwhm's were kept almost constant. If there is the driving force in the direction lateral to the film surface, the fwhm should change. But in fact, the fwhm's stayed almost constant. Thus this result is another proof that the direction of driving force is parallel to the light polarization (z). It should be noted that the trend of the dependence of the size of the deformation on the irradiation intensity is the same as that on exposure time (not shown).

In order to control the light intensity gradient inside a polymer film, we manipulated the refractive index of the material on a film. As the material on the film, we utilized a droplet of glycerin, whose refractive index is 1.47. Since this refractive index is close to that of the PMA-DR1 film (n = 1.67 for 532 nm) compared with air (n = 1.0), the refractive index mismatch between the upper layer of glycerin and the film is reduced compared with the no glycerin case, i.e., air. Thus the light intensity gradient inside the film is expected to change. We prepared the 18 and 60 nm thick films and investigated film thickness dependence with and without glycerin (see Figure 9).

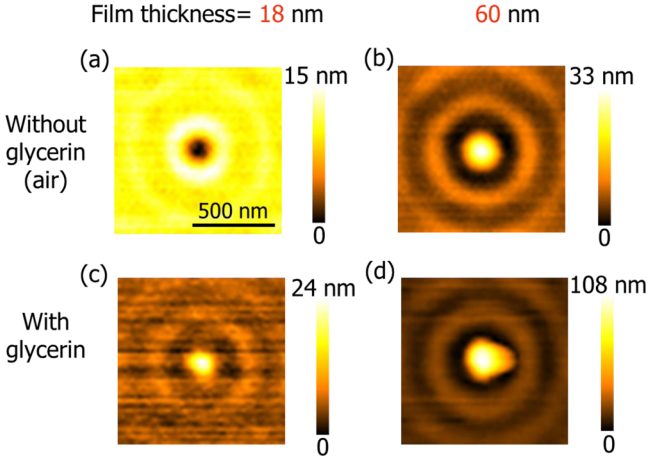

Figure 9. AFM images of the surface deformation induced by E_z in the (a, c) 18 nm and (b, d) 60 nm thick films (c, d) with and (a, b) without glycerin.

The glycerin was completely and cleanly removed by water before AFM observations. We confirmed by the AFM observations that any surface morphology change was not induced in this removing process (not shown). Like the experiments done in Figure 4, the polymer formed a dip at the center of the focused spot when the film thickness is thinner (18 nm), while the polymer formed a protrusion when the film thickness is thicker (60 nm). It is interesting to see that when a droplet of glycerin was put onto the 18 nm film (Figure 9c), the polymer formed a protrusion, a feature that shows a completely opposite direction of polymer movement compared with the no glycerin case (Figure 9a). It is considered from this result that the material's property, such as glass transition temperature (T_g)[27] or isomerization rate,[28] does not change with a change in film thickness; rather, the optical property changes. That is, the light intensity gradient change is mainly responsible for the observed film thickness dependence of the polymer movement. This result demonstrates that upward and downward forces are competing with each other inside the polymer film, and which is stronger is dependent on the light intensity gradient inside the polymer film. We also found that when a droplet of glycerin was put onto the 60 nm film (Figure 9d), the polymer formed a protrusion, like in the no glycerin case (Figure 9b), but the height was increased by almost 3 times (32 nm to 108 nm).

In order to determine the light intensity gradient inside a film, we calculated field distributions in a three-layer system (cover glass/polymer film/air or glycerin). All parameters used in this calculation such as the NA of the objective lens, laser wavelength, film thickness, and refractive index of the materials are the same as the experimental ones. In addition, all optical phenomena, i.e., refraction, reflection, multireflection between the interfaces, and absorption of the film, were taken into account. The focused laser beam is irradiated from the bottom (cover glass side). Figure 10 shows the line plots of $|E_z|^2$ along

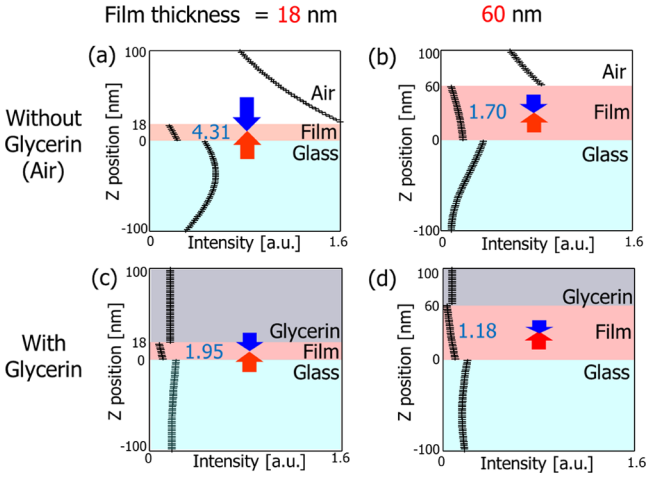

Figure 10. Calculated field distributions of electric field components of E_z created by a focused radially polarized laser beam in the (a, c) 18 nm and (b, d) 60 nm thick films (c, d) with and (a, b) without glycerin. The line plots of $|E_z|^2$ along the optical axis (z) at the center of the focused spot ($x = y = 0$). Calculations shown in (a) to (d) correspond to experimental results of Figure 9a–d, respectively. The upward force indicated by red arrows and the downward force indicated by blue arrows are anisotropic photofluidic force and optical gradient force, respectively. The values indicated by blue letters in each figure are the light intensity gradient, $(d|E_z|^2)/(dz)$ [$\times 10^{-3}$, 1/nm], inside the different thickness films.

the optical axis (z) at the center of the focused spot ($x = y = 0$). Calculations shown in Figure 10a–d correspond to the experimental results of Figure 9a–d, respectively. In all cases E_z is much stronger than $E_{x,y}$, especially at the center of the focused spot ($x = y = 0$), where there is no $E_{x,y}$; thus only E_z is shown in this figure. The values indicated by blue letters in each figure are the light intensity gradient, $d|E_z|^2/dz$ [1/nm], inside the films of different thickness. It is clearly shown that light intensities inside the polymer film gradually decrease from the cover glass side to the polymer film surface for all four cases. It is also shown that the light intensity gradient decreases as the film thickness is increased. These are due to the joint effect of the film absorption and optical interference inside the film. It is clear to see that when a droplet of glycerin is put onto the films, the light intensity gradient inside the films is decreased, i.e., 4.31×10^{-3} [1/nm] to 1.95×10^{-3} [1/nm] for the 18 nm thick film and 1.70×10^{-3} [1/nm] to 1.18×10^{-3} [1/nm] for the 60 nm thick film, since the refractive index mismatch (Δn = 0.20) between glycerin and the polymer film becomes small

dx.doi.org/10.1021/ph400052b | ACS Photonics 2014, 1, 190–197

compared with that (Δn = 0.67) between air and the polymer film.

Here we consider two possible competing forces that were implied by experimental results. One should be anisotropic photofluidic force,[23] which is triggered by trans ↔ cis photoselective isomerization and successive molecular reorientation of azobenzene moieties and induces polymer movement in the polarization direction from the high to the low light intensity region. The other might be optical gradient force,[19,29] which attracts material from the low to the high light intensity region if an irradiation light wavelength corresponds to the right shoulder (or side) of an absorption band. Thus, it is reasonable to think that the upward force (indicated by red arrows) and the downward force (indicated by blue arrows) might correspond to anisotropic photofluidic force and optical gradient force, respectively. In the 18 nm thick film and before putting glycerin onto the film (Figures 9a and 10a), it is considered that downward optical gradient force is stronger than upward anisotropic photofluidic force because a dip was formed in the center of the focused spot. In contrast, after putting glycerin onto the film (Figures 9c and 10c), upward anisotropic photofluidic force is considered to be stronger than downward optical gradient force because a protrusion was formed. It is well known that optical gradient force is proportional to the light intensity gradient,[30] i.e., $F_{grad} \propto dI/dz$ where I is light intensity and z is the z-axis. By using glycerin the light intensity gradient was decreased by a factor of ∼2, i.e., from 4.31 × 10^{-3} [1/nm] to 1.95 × 10^{-3} [1/nm]; therefore optical gradient force is also decreased by a factor of ∼2. If we assume that anisotropic photofluidic force is also proportional to light intensity gradient, i.e., $F_{fluid} \propto dI/dz$, anisotropic photofluidic force should also decrease by a factor of ∼2. This means that optical gradient force is still stronger than anisotropic photofluidic force, and a dip should be formed after putting glycerin on the film. In fact, the opposite behavior was observed, i.e., a protrusion was formed (Figure 9c). Thus we could assume that anisotropic photofluidic force has a nonlinear response to light intensity gradient. Currently we do not know the detailed dependence of anisotropic photofluidic force on light intensity gradient, and this will be our next target, but for simplicity, we assume $E_{fluid} \propto (dI/dz)^{\alpha}$ where α is less than 1 ($\alpha < 1$). Figure 11 shows the relationship between driving forces (F_{grad}, F_{fluid}) and light intensity gradient (dI/dz) where we set α to 0.5. It is clear that at low light intensity gradient, anisotropic photofluidic force is stronger than optical gradient force (which induces a protrusion), while at high light intensity gradient, optical gradient force is stronger than anisotropic photofluidic force (which induces a dip). It is important to say that there is a balance (cross) point where anisotropic photofluidic force is equal to optical gradient force, and thus polymer movement is not induced. We already know that in the 37 nm thick film, polymer movement was not induced (see Figure 5), so the 37 nm film thickness corresponds to this balance point. We calculated the light intensity gradient inside the 37 nm polymer film, and we found that this balanced value of the light intensity gradient is 3.03 × 10^{-3} [1/nm]. In the 60 nm thick film, the light intensity gradient before putting glycerin onto the film is calculated to be 1.70 × 10^{-3} [1/nm] (Figure 10b), which is smaller than the balanced value of 3.03 × 10^{-3} [1/nm]. On the basis of our assumption discussed above, anisotropic photofluidic force is stronger than optical gradient force in this film thickness; thus the protrusion was induced (Figure 9b). By putting glycerin on the film, the light intensity gradient is decreased to 1.18 × 10^{-3} [1/nm] (Figure 10d). Accordingly, both anisotropic photofluidic force and optical gradient force are decreased, but the degree of decrease in optical gradient force is bigger than that in anisotropic photofluidic force (see Figure 11). This leads to a stronger upward net force compared with the no glycerin case, which results in the enhancement of the height of the protrusion (Figure 9d).

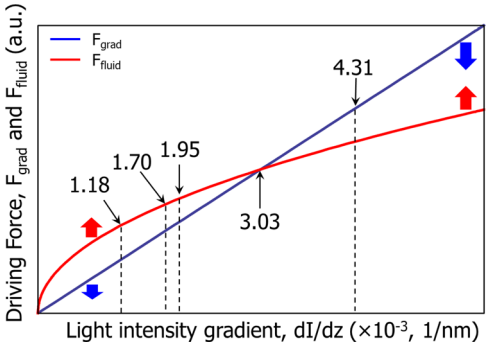

Figure 11. Relationship between driving force (F_{grad}, F_{fluid}) and light intensity gradient (dI/dz) where α is set to 0.5. The blue and the red lines are optical gradient force and anisotropic photofluidic force, respectively. The values are the light intensity gradient.

We studied irradiation wavelength dependence of polymer movement. The direction of polymer movement induced by anisotropic photofluidic force is independent of the irradiation wavelength, but the direction of polymer movement induced by optical gradient force is dependent on irradiation wavelength. If an irradiation light wavelength corresponds to the right (or left) of an absorption maximum, optical gradient force attracts material from the low (or high) to the high (or low) light intensity region.[19,29] Thus depending on the wavelength of the irradiation light, the direction of polymer movement induced by optical gradient force becomes completely opposite. In this experiment, we changed the irradiation wavelength from 532 nm to 460 nm. The irradiation wavelength of 460 nm corresponds to the left shoulder of the absorption band (λ_{max} = 467 nm) of the side-chain azobenzene moiety. Thus the direction of optical gradient force should change from downward to upward if the optical gradient force acts on the side-chain azobenzene moiety. This gives formation of a protrusion at the center of a focused spot even for a thinner polymer film because the direction of the joint force between anisotropic photofluidic force and optical gradient force is always upward, while irradiation at 532 nm induced a dip for the thinner polymer film (Figure 4a). Figure 12 shows the AFM images of the surface deformation induced by irradiation at 460 nm onto (a) 24 and (b) 40 nm thick films. It is clear to see that

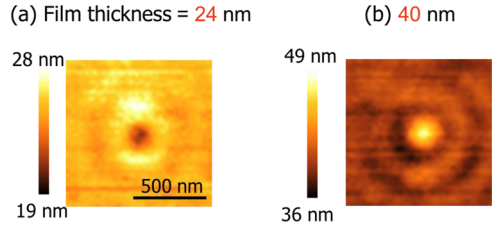

Figure 12. AFM images of the surface deformation induced by E_z in the (a) 24 nm and (b) 40 nm thick films with 460 nm light irradiation.

dx.doi.org/10.1021/ph400052b | ACS Photonics 2014, 1, 190−197

the dip and the protrusion were formed on thin (24 nm) and thick (40 nm) polymer films, respectively. This result shows that the trend of surface topology change was found to be the same for irradiation with both 460 and 532 nm light, i.e., independent of the irradiation wavelength. Therefore, we can assume that optical gradient force exerted on not the side-chain of the azobenzene moiety but the main chain of the polymer contributes to the polymer movement, because the absorption band of the main chain of the polymer is located in the UV region (λ_{max} = 211 nm), where both 460 and 532 nm wavelengths correspond to the right side of the absorption band of the main chain polymer. It is reasonable to think that the energy of the optical gradient force exerted on the side-chain of the azobenzene moiety is dissipated to movement of not the polymer but the azobenzene moiety itself in the local free volume because the azobenzene moiety is not rigidly connected to the main chain of the polymer.

CONCLUSION

We studied surface deformations induced in an azo-polymer film by a focused light spot having longitudinal fields (E_z). We found that the deformation patterns induced by E_z were strongly dependent on the film thickness and refractive index of the material on the film. We calculated the light field distribution inside the polymer film, and by comparing the experimental results we found that both anisotropic photo-fluidity force and optical gradient force might play important roles in the light-induced polymer movement by E_z. In addition, we found by changing the wavelength of the irradiation light that optical gradient force exerted on not the side-chain of the azobenzene moiety but the main chain of the polymer contributes to the polymer movement.

AUTHOR INFORMATION

Corresponding Author

*E-mail: ishitobi@ap.eng.osaka-u.ac.jp.

Notes

The authors declare no competing financial interest.

ACKNOWLEDGMENTS

This work was supported by a Grant-in-Aid for Young Scientists (B) (No. 23760054) and a Grant-in-Aid for Scientific Research in Priority Areas "New Frontiers in Photochromism (No. 471)" both from the Ministry of Education, Culture, Sports, Science and Technology (MEXT), Japan.

REFERENCES

(1) Kravchenko, A.; Shevchenko, A.; Ovchinnikov, V.; Priimagi, A.; Kaivola, M. Optical interference lithography using azobenzene-functionalized polymers for micro- and nanopattering of silicon. *Adv. Mater.* **2011**, *23*, 4174−4177.

(2) Sekkat, Z.; Kawata, S. Laser nanofabrication in photoresists and azopolymers. *Laser Photon. Rev.* **2014**, *8*, 1−26.

(3) Hubert, C.; Rumyantseva, A.; Lerondel, G.; Grand, J.; Kostcheev, S.; Billot, L.; Vial, A.; Bachelot, R.; Royer, P.; Chang, S. H.; Gray, S. K.; Wiederrecht, G. P.; Schatz, G. C. Near-field photochemical imaging of nobel metal nanostructures. *Nano Lett.* **2005**, *5*, 615−619.

(4) Plain, J.; Wiederrecht, G. P.; Gray, S. K.; Royer, P.; Bachelot, R. Multiscale optical imaging of complex fields based on the use of azobenzene nanomotors. *J. Phys. Chem. Lett.* **2013**, *4*, 2124−2132.

(5) Jiang, X. L.; Li, L.; Kumar, J.; Kim, D. Y.; Shivshankar, V.; Tripathy, S. K. Polarization dependent recordings of surface relief gratings on azobenzene containing polymer films. *Appl. Phys. Lett.* **1996**, *68*, 2618−2620.

(6) Rochon, P.; Batalla, E.; Natansohn, A. Optically induced surface gratings on azoaromatic polymer films. *Appl. Phys. Lett.* **1995**, *66*, 136−138.

(7) Kim, D. Y.; Tripathy, S. K.; Li, L.; Kumar, J. Laser-induced holographic surface relief gratings on nonlinear optical polymer films. *Appl. Phys. Lett.* **1995**, *66*, 1166−1168.

(8) Pedersen, T. G.; Johansen, P. M.; Holme, N. C. R.; Ramanujam, P. S. Mean-field theory of photoinduced formation of surface reliefs in side-chain azobenzene polymers. *Phys. Rev. Lett.* **1998**, *80*, 89−92.

(9) Lefin, P.; Fiorini, C.; Nunzi, J. M. Anisotropy of the photoinduced translation diffusion of azo-dyes. *Opt. Mater.* **1998**, *9*, 323−328.

(10) Labarthet, F. L.; Buffeteau, T.; Sourissean, C. Analyses of the diffraction efficiencies, birefringence, and surface relief gratings on azobenzene-containing polymer films. *J. Phys. Chem. B* **1998**, *102*, 2654−2662.

(11) Barrett, C. J.; Rochon, P. L.; Natansohn, A. L. Model of laser-driven mass transport in thin films of dye-functionalized polymers. *J. Chem. Phys.* **1998**, *109*, 1505−1516.

(12) Sumaru, K.; Yamanaka, T.; Fukuda, T.; Matsuda, H. Photoinduced surface relief gratings on azopolymer films: Analysis by a fluid mechanics model. *Appl. Phys. Lett.* **1999**, *75*, 1878−1880.

(13) Yager, K. G.; Barrett, C. J. Temperature modeling of laser-irradiated azo-polymer thin films. *J. Chem. Phys.* **2004**, *120*, 1089−1096.

(14) Saphiannikova, M.; Geue, T. M.; Henneberg, O.; Morawetz, K.; Pietsch, U. Linear viscoelastic analysis of formation and relaxation of azobenzene polymer gratings. *J. Chem. Phys.* **2004**, *120*, 4039−4045.

(15) Barada, D.; Itoh, M.; Yatagai, T. Computer simulation of photoinduced mass transport on azobenzene polymer films by particle method. *J. Appl. Phys.* **2004**, *96*, 4204−4210.

(16) Bian, S.; Williams, J. M.; Kim, D. Y.; Lin, L.; Balasubramanian, S.; Kumar, J.; Tripathy, S. Photoinduced surface deformations on azobenzene polymer films. *J. Appl. Phys.* **1999**, *86*, 4498−4508.

(17) Gilbert, Y.; Bachelot, R.; Royer, P.; Bouhelier, A.; Wiederrecht, G. P.; Novotny, L. Longitudinal anisotropy of the photoinduced molecular migration in azobenzene polymer films. *Opt. Lett.* **2006**, *31*, 613−615.

(18) Grosjean, T.; Courjon, D. Photopolymers as vectorial sensors of the electric field. *Opt. Express* **2006**, *14*, 2203−2210.

(19) Ishitobi, H.; Tanabe, M.; Sekkat, Z.; Kawata, S. The anisotropic nanomevement of azo-polymers. *Opt. Express* **2007**, *15*, 652−659.

(20) Grosjean, T.; Courjon, D.; Bainier, C. Smallest lithographic marks generated by optical focusing systems. *Opt. Lett.* **2007**, *15*, 976−978.

(21) Ishitobi, H.; Shoji, S.; Hiramatsu, T.; Sun, H. B.; Sekkat, Z.; Kawata, S. Two-photon induced polymer nanomovement. *Opt. Express* **2008**, *16*, 14106−14114.

(22) Ambrosio, A.; Marrucci, L.; Borbone, F.; Roviello, A.; Maddalena, P. Light-induced spiral mass transport in azo-polymer films under vortex-beam illumination. *Nat. Commun.* **2012**, *3*, 1−9.

(23) Karageorgiev, P.; Neher, D.; Schulz, B.; Stiller, B.; Pietsch, U.; Giersig, M.; Brehmer, L. From anisotropic photo-fluidity towards nanomanipulation in the optical near-field. *Nat. Mater.* **2005**, *4*, 699−703.

(24) Sekkat, Z.; Knoll, W. *Photoreactive Organic Thin Films*; Academic Press: New York, 2002.

(25) Sekkat, Z.; Wood, J.; Knoll, W.; Volksen, W.; Miller, R. D. Light-induced orientation in a high glass transition temperature polyimide with polar azo dyes in the side chain. *J. Opt. Soc. Am. B* **1996**, *13*, 1713−1724.

(26) Ishitobi, H.; Nakamura, I.; Hayazawa, N.; Sekkat, Z.; Kawata, S. Orientational imaging of single molecules by using azimuthal and radial polarizations. *J. Phys. Chem. B* **2010**, *114*, 2565−2571.

(27) Alcoutlabi, M.; McKenna, G. B. Effects of confinement on material behaviour at the nanometre size scale. *J. Phys.: Condens. Matter* **2005**, *17*, R461−R524.

(28) Tateishi, T.; Tanaka, K.; Nagamura, T. Film thickness dependence of photoisomerization for azobenzene chromophores

tagged to polystyrene with various molecular weights. *Trans. Mater. Res. Soc. Jpn.* **2005**, *30*, 643−646.
(29) Ishitobi, H.; Tanabe, M.; Sekkat, Z.; Kawata, S. Nanomovement of azo polymers induced by metal tip enhanced near-field irradiation. *Appl. Phys. Lett.* **2007**, *91*, 091911.
(30) Ashkin, A.; Dziedzic, J. M.; Bjorkholm, J. E.; Chu, S. Observation of a single-beam gradient force optical trap for dielectric particles. *Opt. Lett.* **1986**, *11*, 288−290.